COSMOLOGICAL RELIC DENSITY FROM MINIMAL SUPERGRAVITY WITH IMPLICATIONS FOR COLLIDER PHYSICS

Howard Baer and Michal Brhlik

Department of Physics, Florida State University, Tallahassee, FL 32306 USA

(November 1, 2021)

Abstract

Working within the framework of the minimal supergravity model with gauge coupling unification and radiative electroweak symmetry breaking, we evaluate the cosmological relic density from lightest neutralinos produced in the early universe. Our numerical calculation is distinct in that it involves direct evaluation of neutralino annihilation cross sections using helicity amplitude techniques, and thus avoids the usual expansion as a power series in terms of neutralino velocity. Thus, our calculation includes relativistic Boltzmann averaging, neutralino annihilation threshold effects, and proper treatment of integration over Breit-Wigner poles. We map out regions of parameter space that give rise to interesting cosmological dark matter relic densities. We compare these regions with recent calculations of the reach for supersymmetry by LEP2 and Tevatron Main Injector era experiments. The cosmologically favored regions overlap considerably with the regions where large trilepton signals are expected to occur at the Tevatron. The CERN LHC pp collider can make a thorough exploration of the cosmologically favored region via gluino and squark searches. In addition, over most of the favored region, sleptons ought to be light enough to be detectable at both LHC and at a $\sqrt{s} = 500 \text{ GeV } e^+e^- \text{ collider.}$

I. INTRODUCTION

The Minimal Supersymmetric Standard Model [1] (MSSM) is one of the leading candidate theories for physics beyond the Standard Model (SM). The MSSM is a globally supersymmetric version of the SM, where supersymmetry breaking is implemented by the explicit introduction of soft-supersymmetry breaking terms. The MSSM is minimal in the sense that the fewest number of additional new particles and interactions are incorporated which are consistent with phenomenology. In particular, possible baryon (B) and lepton (L) number violating interactions are excluded from the superpotential (the presence of both B and L violating interactions can lead to catastrophic proton decay rates). As a result, there exists a conserved R-parity, where the multiplicative quantum number R=+1 for ordinary particles, and R=-1 for superpartners. A consequence of R-parity conservation is that the lightest supersymmetric particle (LSP) is absolutely stable. Theoretical prejudice coupled with experimental constraints strongly favor a color and charge neutral LSP [2]. In addition, in the MSSM, the LSP is strongly favored to be the massive, weakly interacting lightest neutralino Z_1 [3,4]. Z_1 's, if they exist, would have been abundantly produced in the early universe; if so, then relic neutralinos could well make up the bulk of the dark matter in the universe today [5,6].

In this paper, we restrict ourselves to the framework of the low energy effective Lagrangian which is expected to result from, for instance, supergravity grand unified models [7]. In these models, it is assumed that supersymmetry is broken in a hidden sector of the theory. Supersymmetry breaking is then communicated to the observable sector via gravitational interactions, leading to a common mass m_0 for all scalar particles, a common mass $m_{1/2}$ for all gauginos, a common trilinear coupling A_0 , and a bilinear coupling B_0 . These soft supersymmetry breaking parameters are induced at energy scales at or beyond the unification scales, but with (theoretically motivated) values typically in the range 100-1000 GeV. The resulting theory, the MSSM with universal soft breaking terms, is then regarded as an effective theory with Lagrangian parameters renormalized at an ultrahigh scale $M_X \sim M_{GUT} - M_{Planck}$, and valid only below this scale. The corresponding weak scale sparticle couplings and masses can then be calculated by evolving 26 parameters via renormalization group equations [8] from the unification scale to the weak scale. An elegant by-product [9] of this mechanism is that one of the Higgs boson mass squared terms is driven negative, resulting in a breakdown of electroweak symmetry. The radiative electroweak symmetry breaking constraint allows one to essentially eliminate B in favor of $\tan \beta$ (the ratio of Higgs field vev's), and to calculate the magnitude of the superpotential Higgs mixing term μ in terms of M_Z (where we actually minimize the full one-loop effective potential). The model is then specified by only four SUSY parameters (in addition to SM masses and couplings). A hybrid set consisting of the common GUT scale scalar mass m_0 , common gaugino mass $m_{1/2}$, common SUSY-breaking trilinear coupling A_0 , along with the weak scale value of $\tan \beta$ proves to be a convenient choice. In addition, the sign of μ must be stipulated. These parameters fix the weak scale masses and couplings of all the sparticles [10].

The matter density of the universe ρ is usually parametrized [5,6] in terms of $\Omega = \rho/\rho_c$, where $\rho_c = 3H_0^2/8\pi G_N \simeq 1.88 \times 10^{-29}h^2$ g/cm³, and h, the Hubble scaling constant, is related to the Hubble constant H_0 by $H_0 = 100h$ km/sec/Mpc. Here h parametrizes our

ignorance of the true value of H_0 , so that $0.5 \lesssim h \lesssim 0.8$. Measurements of galactic rotation curves suggest $\Omega \sim 0.03-0.1$, compared to a luminous matter density of $\Omega_{lum.} \lesssim 0.01$. Galactic clustering and galactic flows suggest even larger values of $\Omega \sim 0.2-1$. Finally, the theoretically attractive inflationary cosmological models require a flat universe with $\Omega = 1$. Meanwhile, estimates of the baryonic contribution to the matter density of the universe from Big-Bang nucleosynthesis suggest that $\Omega_{baryonic} \sim 0.01-0.1$. These analyses and estimates suggest that the bulk of matter in the universe is (non-baryonic) dark matter. Finally, analyses of structure formation in the universe in light of the COBE measurements of anisotropies in the cosmic microwave background radiation suggest that dark matter may be made of $\sim 60\%$ cold-dark matter (weakly interacting massive particles or WIMPS, such as the lightest neutralino \tilde{Z}_1), $\sim 30\%$ hot dark matter (such as relic neutrinos), and $\sim 10\%$ baryonic matter. This is the so-called "mixed dark matter" scenario.

The central idea [5] behind relic density calculations is that in the very early universe, neutralinos were being created and annihilated, but that they were in a state of thermal equilibrium with the cosmic soup. As the universe expanded and cooled, temperatures dropped low enough that neutralinos could no longer be produced $(T \lesssim m_{\widetilde{Z}_1})$, although they could still annihilate with one another, at a rate governed by the total neutralino pair annihilation cross section, and the neutralino number density. Ultimately, as the universe expanded further, the expansion rate outstripped the annihilation rate, thus freezing out the remaining neutralino population of the universe, and locking in a neutralino relic density. Our goal in this paper is to carry out estimates of the neutralino relic density expected from the minimal SUGRA model. One solid constraint on supersymmetric models with relic dark matter particles comes from the age of the universe, which ought to be greater than 10 (15) Gyrs; this implies $\Omega h^2 < 1$ (0.25). Thus, models with too large a relic density would yield too young of a universe, in violation at least with the age of the oldest stars in globular clusters. Furthermore, models with $\Omega h^2 < 0.025$ would not even be able to account for the dark matter needed to explain galactic rotation: such models would be considered cosmologically uninteresting. Models with intermediate values of $0.025 \lesssim \Omega h^2 \lesssim 1$ are considered cosmologically interesting, as they might explain galactic rotation and clustering, or might even make up the matter density needed for inflationary cosmology, given a colddark matter (CDM: $\Omega h^2 \sim 0.25 - 0.64$) or mixed hot/cold dark matter scenario (MDM: $\Omega h^2 \sim .15 - .4$).

Following the procedures outlined by Lee and Weinberg [11], many groups have calculated the relic neutralino abundance [12–19]. Early works involved calculating the most important neutralino annihilation channels, usually assuming the LSP was a photino. Later studies included various improvements, including more annihilation channels, more general neutralino mixings, and more realistic supersymmetric particle spectra. A common thread amongst many papers was the calculation of the Boltzmann-averaged quantity $\sigma \times v$ using a power series expansion in velocity. Such an approach was shown to be inaccurate when relativistic effects were important, when annihilation proceeded through s-channel poles, when threshold effects were important, or when co-annihilation processes occured [20,21]. Many recent calculations have included some or all of these effects.

We have several goals in mind for the present paper.

• We wish to present reliable calculations for the neutralino relic density in supersymmetric models. To this end we evaluate $all\ 2 \rightarrow 2$ neutralino annihilation diagram

amplitudes numerically as complex numbers, without approximation. We perform Boltzmann averaging using the Gondolo-Gelmini formalism [21]. This takes into account relativistic thermal averaging, while our numerical helicity amplitude technique avoids the usual uncertainties inherent in the velocity expansion, so that Breit-Wigner poles and threshold effects are fully accounted for. Co-annihilation can occur when the two lightest superpartners are very close in mass—this situation rarely occurs within the SUGRA framework adopted in this paper, and hence we ignore it.

- We present results in the well-motivated SUGRA framework, which includes gauge coupling unification, Higgs mass radiative corrections [22], and radiative electroweak symmetry breaking using the one-loop effective potential [23].
- Our results for the relic density calculation can be directly related to recent calculations for various supersymmetry signals expected at the LEP2 [24,25], Tevatron [26–29] and LHC colliders [30,31]. In particular, relic density calculations have a preference for light sleptons. Such light sleptons may well be observable at LEP2 or LHC colliders, and yield enhanced rates for $\widetilde{W}_1\widetilde{Z}_2 \to 3\ell$ states at the Tevatron collider [32].

To accommodate these goals, we present in Sec. II various details of our relic density calculation, including those peculiar to the present approach. In Sec. III, we present numerical results for our relic density calculations in the m_0 vs. $m_{1/2}$ plane of the minimal SUGRA model. In Sec. IV, these results are explicitly compared to expectations for minimal SUGRA at various collider experiments, as worked out in a series of previous papers. Finally, in Sec. V we present an overview and some conclusions.

II. CALCULATIONAL DETAILS

We begin our determination of the neutralino relic density from minimal supergravity by selecting a point in the SUGRA parameter space

$$m_0, m_{1/2}, \tan \beta, A_0 \text{ and } sign(\mu),$$
 (2.1)

where in addition we take the top quark mass $m_t = 170$ GeV. The 26 renormalization group equations are iteratively run between the weak scale and the GUT scale, which is defined as the point where the U(1), SU(2) and SU(3) gauge couplings unify, and is typically $M_X \sim 2 \times 10^{16}$ GeV. We use 2-loop RGE equations for gauge and Yukawa couplings (with SUSY particle threshold effects), but only 1-loop equations for the running of the various soft breaking terms. The 1-loop effective Higgs potential is minimized to enforce radiative electroweak symmetry breaking. Our procedure has been described in more detail in Ref. [33], and has been incorporated into the event generator ISAJET [34]. At this point, a correlated sparticle mass spectrum and couplings emerge from our input point in SUGRA parameter space.

The next step in our computation, after obtaining the superparticle spectrum, is to evaluate the neutralino relic density by solving the Boltzmann equation as formulated for a Friedmann-Robertson-Walker cosmology [5]. Central to the evaluation of the relic density is the computation of the fully relativistic, thermally averaged neutralino annihilation cross section times velocity, defined as

$$<\sigma v_{Mol}>(T)=rac{\int \sigma v_{Mol}e^{-E_1/T}e^{-E_2/T}d^3p_1d^3p_2}{\int e^{-E_1/T}e^{-E_2/T}d^3p_1d^3p_2},$$
 (2.2)

where p_1 (E_1) and p_2 (E_2) are the momentum and energy of the two colliding particles in the cosmic, co-moving frame of reference, and T is the temperature. The above expression has been reduced to a one-dimensional integral by Gondolo and Gelmini [21], which yields

$$<\sigma v_{Mol}>(x)=\frac{1}{4xK_2^2(\frac{1}{x})}\int_2^\infty da\sigma(a)a^2(a^2-4)K_1(\frac{a}{x}),$$
 (2.3)

where $x = \frac{T}{m_{\widetilde{Z}_1}}$, $a = \frac{\sqrt{s}}{m_{\widetilde{Z}_1}}$, \sqrt{s} is the subprocess energy, and K_i are modified Bessel functions of order i.

We evaluate the neutralino annihilation cross section for $\tilde{Z}_1\tilde{Z}_1 \to f_1f_2$ as

$$d\sigma(a) = \frac{1}{32\pi s} \frac{\lambda^{\frac{1}{2}}(s, m_{f_1}^2, m_{f_2}^2)}{\lambda^{\frac{1}{2}}(s, m_{\widetilde{Z}_1}^2, m_{\widetilde{Z}_1}^2)} \overline{\Sigma} |\mathcal{M}|^2 d\cos\theta,$$
(2.4)

where $\overline{\Sigma}|\mathcal{M}|^2$ is the spin summed and averaged squared matrix element. Our calculation of the relic density is distinct in that we evaluate \mathcal{M} for all Feynman diagrams listed in Table 1 as complex numbers, using the HELAS [35] helicity amplitude subroutine package. Thus, our approach avoids the usual uncertainties associated with the expansion of cross section in terms of a power series in velocity. The integration over $\cos \theta$ is performed numerically using Gaussian quadratures.

To evaluate the neutralino relic density, the freeze out temperature x_F is needed. The standard procedure here to iteratively solve the freeze out relation

$$x_F^{-1} = \log\left[\frac{m_{\widetilde{Z}_1}}{2\pi^3}\sqrt{\frac{45}{2g_*G_N}} < \sigma v_{Mol} >_{x_F} x_F^{\frac{1}{2}}\right],$$
 (2.5)

by starting with a trial value $x_F = \frac{1}{20}$. In the above, g_* is the effective number of degrees of freedom at $T = T_F$ ($\sqrt{g_*} \simeq 9$), and G_N is Newton's constant.

Finally, the relic density can be calculated from

$$\Omega h^2 = \frac{\rho(T_0)}{8.0992 \times 10^{-47} \text{ GeV}^4},\tag{2.6}$$

where

$$\rho(T_0) \simeq 1.66 \times \frac{1}{M_{Pl}} \left(\frac{T_{m_{\widetilde{Z}_1}}}{T_{\gamma}}\right)^3 T_{\gamma}^3 \sqrt{g_*} \frac{1}{\int_0^{x_F} \langle \sigma v_{Mol} \rangle dx}.$$
 (2.7)

To evaluate the integral in the above expression, we expand the modified Bessel functions in Eq. 2.3 as power series in x, and then integrate over x. The result is

$$\int_0^{x_F} \langle \sigma v_{Mol} \rangle dx = \frac{1}{8\pi} \int_2^{\infty} da \sigma(a) a^{\frac{3}{2}} (a^2 - 4) F(a), \tag{2.8}$$

where

$$\begin{split} F(a) &= \sqrt{\frac{\pi}{a-2}} \left\{ 1 - Erf(\sqrt{\frac{a-2}{x_F}}) \right\} + \\ &\quad 2(\frac{3}{8a} - \frac{15}{4}) \left\{ \sqrt{x_F} e^{-\frac{a-2}{x_F}} - \sqrt{\pi(a-2)}(1 - Erf(\sqrt{\frac{a-2}{x_F}})) \right\} + \\ &\quad \frac{2}{3} (\frac{285}{32} - \frac{45}{32a} - \frac{15}{18a^2}) \times \\ &\quad \left\{ e^{-\frac{a-2}{x_F}} \left[x_F^{\frac{3}{2}} - 2(a-2)\sqrt{x_F} \right] + 2\sqrt{\pi}(a-2)^{\frac{3}{2}}(1 - Erf(\sqrt{\frac{a-2}{x_F}})) \right\}. \end{split}$$

In the above, virtually all the contribution to the integral comes from x < 2.5. We integrate the above expression numerically with Gaussian quadratures, taking care to scan finely the regions with a Breit-Wigner pole. In the region of a pole, the domain of integration must be broken into very tiny intervals, and obtaining convergence for a single point in parameter space can take up to several hours of CPU time on a DEC ALPHA.

III. RESULTS FROM RELIC DENSITY CALCULATION

Our first numerical results for the relic density from minimal SUGRA models are given in Fig. 1, where we plot contours of the neutralino relic density Ωh^2 in the m_0 vs. $m_{1/2}$ parameter plane, where we take $A_0 = 0$, $\tan \beta = 2$, $\mu < 0$ and $m_t = 170$ GeV. Changes in the A_0 parameter mainly affect 3rd generation sparticle masses, and consequently result in only small changes in the relic density. The regions labelled TH are excluded by theoretical considerations: either there is a charged or colored LSP (or the $\tilde{\nu}$ is LSP), or the radiative electroweak symmetry breaking constraint breaks down. The region labelled by EX corresponds to parameter space already excluded by SUSY searches at LEP or Fermilab Tevatron experiments [33].

In almost all of the plane, we find $\Omega h^2 > 0.025$, *i.e.* large enough to explain the galactic rotation curves. However, the region to the right of the $\Omega h^2 = 1$ contour is certainly excluded in that the age of the universe would be younger than 10 Gyrs. Meanwhile, a dominantly CDM inflationary universe would lie in between the $\Omega h^2 = 0.25 - 0.75$ contours. The COBE favored MDM inflationary universe would lie between the $\Omega h^2 = 0.15 - 0.4$ contours. For this latter favored region, $m_{1/2}$ is bounded by $m_{1/2} \lesssim 400$ GeV (corresponding to $m_{\tilde{g}} \lesssim 1000$ GeV), and $m_0 < 150$ GeV, unless the gluino is very light ($m_{\tilde{g}} \simeq 300$ GeV). (For comparison, various SUSY particle mass contours for the same parameter choices are listed in Refs. [33,28,30].) We find in general that large values of $m_0 \gtrsim 350$ GeV (corresponding to $m_{\tilde{\ell}} \gtrsim 250$ GeV) yield too young a universe (due to suppression of t-channel slepton exchange diagrams), except for the two narrow corridors in the lower right region of the figure. The upper of the two corridors corresponds to neutralino annihilation through the Z pole, so the relic density is largely reduced by Z mediated s-channel annihilation diagrams. The lower of the two corridors corresponds to annihilation through an s-channel light Higgs h pole— in this case, the relic density falls rapidly to values even below $\Omega h^2 \sim 0.025$.

A qualitative feel for the relative importance of different annihilation channels can be gleaned from Fig. 2. Here we plot for m_0 fixed at 200 GeV, as a function of $m_{1/2}$, the thermally averaged annihilation cross section times velocity, integrated over temperature,

which enters into the relic density calculation (Eq. 2.8). Larger cross sections correspond to smaller relic densities. As $m_{1/2}$ increases, the first pole we come to is annihilation via s-channel h, where $\tilde{Z}_1\tilde{Z}_1\to b\bar{b}$ dominates. In these plots, $m_{\tilde{Z}_1}$ scales with $m_{1/2}$, and at the Higgs pole in this plot (on the edge of exclusion by LEP Higgs search experiments), $m_{\tilde{Z}_1}\simeq 30$ GeV and $m_{\tilde{W}_1}\simeq 70$ GeV. As one moves to higher $m_{1/2}$, annihilation through the Z pole is reached, which is dominated by $\tilde{Z}_1\tilde{Z}_1\to d\bar{d}$, $s\bar{s}$, and $b\bar{b}$. For values of $m_{1/2}$ away from poles, annihilation via t-channel slepton and sneutrino exchange dominates. For even higher $m_{1/2}$ values, annihilation into channels such as hh, Zh, WW and ZZ open up, but never dominate for the parameter choices in this plot. Annihilation into other channels such as HA, AA, HH amd H^+H^- are included in our calculation, but unimportant given our SUGRA sparticle mass spectrum, which yields very large masses for Higgs bosons other than h. The onset of the $\tilde{Z}_1\tilde{Z}_1\to t\bar{t}$ can be detected in the $\tilde{Z}_1\tilde{Z}_1\to \Sigma u_i\bar{u}_i$ curve around $m_{1/2}\sim 400$ GeV.

If we plot the relic density for the same parameter choices, but flip the sign of μ , so that $\mu > 0$, then we obtain the results of Fig. 3. The relic density contours in this case are similar to those of Fig. 1 for large values of $m_{1/2}$, where annihilation dominantly occurs via slepton exchange. The kink in the contours is due to the onset of the $\tilde{Z}_1\tilde{Z}_1 \to t\bar{t}$ channel. In this case, annihilation through t-channel \tilde{t}_1 exchange makes a large contribution to the total annihilation cross section. For smaller values of $m_{1/2}$, in contrast to Fig. 1, we find only one corridor extending to large m_0 where the relic density drops to cosmologically un-interesting values. In this case, the Z and h poles very nearly overlap for $m_{\tilde{Z}_1} \sim 46$ GeV. This can be seen in more detail in Fig. 4, where again we show the thermally averaged cross section versus $m_{1/2}$, for $m_0 = 200$ GeV.

Finally, we show again the neutralino relic density Ωh^2 in the m_0 vs. $m_{1/2}$ plane for the same parameter choices as Fig. 1, except now we take a large value of $\tan \beta = 10$. For this case, we note the rather broad band at $m_{1/2} \sim 100-140$ GeV, where $\Omega h^2 < 0.025$ - too low to explain even the galactic rotation curves, and due again to annihilation through the s-channel graphs. In fact, inflationary models, which require $\Omega h^2 \gtrsim 0.15$, are only allowed if $m_{1/2} > 150$ GeV, corresponding to $m_{\tilde{g}} > 400$ GeV. In this plot, there is a significant region extending to large values of m_0 , corresponding to large $m_{\tilde{q}}$ and large $m_{\tilde{\ell}}$, for $m_{1/2} \sim 150-190$ GeV. The contributing thermally averaged subprocess cross sections are again shown in Fig. 6 for $m_0 = 200$ GeV. In this plot, the Z pole annihilation channel occurs at $m_{1/2} \simeq 110$ GeV, followed by the Higgs pole at $m_{1/2} \simeq 130$ GeV. The rough overlap of these two pole contributions leads to the single broad corridor of low Ωh^2 shown in Fig. 5.

IV. IMPLICATIONS FOR SUSY SEARCHES AT COLLIDERS

Recently, various papers have been written on the prospects for supersymmetry at the LEP2 e^+e^- collider [24,25], the Fermilab Tevatron $p\bar{p}$ collider [32,26–29] and the CERN LHC pp collider [30,31]. Our objective in this section is to assess the prospects for discovery of SUGRA at hadron and e^+e^- colliders, given the additional constraints from requiring a reasonable value for the neutralino relic density. We mainly focus on the collider results of Refs. [25,26,28,30,31,39], since they were performed in a consistent framework, in the same m_0 vs. $m_{1/2}$ plane.

In Fig. 7, we again show the neutralino relic density contours in the m_0 vs. $m_{1/2}$ parameter plane, for the same parameter choices as in Fig. 1. In addition, we have added on contours for SUSY discovery at various colliders. Supersymmetric particles ought to be discoverable at LEP2 operating at $\sqrt{s} = 190$ GeV, with integrated luminosity $\int \mathcal{L}dt = 300$ fb⁻¹ below the contour labelled LEP2 [25]. The lower-left bulge in the LEP2 contour is where sleptons ought to be detectable, while beneath the contour running along $m_{1/2} \simeq 100$ GeV (which runs through the neutralino Z-pole annihilation region), charginos ought to be detectable. By comparing, we see that the region accessible by LEP2 generally has $\Omega h^2 < 0.15$ i.e. not the most cosmologically favored region, but with enough dark matter to explain galactic rotation. However, the contour labelled with LEP2-Higgs shows the reach of LEP2 for the light SUSY Higgs boson h, which is just below $m_{1/2} \sim 400$ GeV. This region completely encloses the favored MDM region. The implication is that if MDM explains dark matter in the universe, and if $\tan \beta$ is small and $\mu < 0$, then LEP2 ought to discover at least the light SUSY Higgs boson.

The dashed contour labelled Tevatron is a composite of the reach of Tevatron Main Injector era ($\sqrt{s}=2$ TeV; $\int \mathcal{L}dt=1$ fb⁻¹ integrated luminosity) experiments for multijet+ E_T events [26], and mainly, for $\widetilde{W}_1\widetilde{Z}_2 \to 3\ell$ events [28]. We see that the largest reach by Tevatron experiments occurs exactly in the cosmologically favored MDM region, and can reach to $m_{1/2} \sim 160$ GeV, corresponding to $m_{\tilde{g}} \sim 440$ GeV. This is no accident: a reasonable neutralino annihilation cross section generally requires $m_{\tilde{\ell}} \lesssim 200$ GeV; these lighter sleptons give rise to enhanced leptonic decay of neutralinos, leading to large rates for $\widetilde{W}_1\widetilde{Z}_2 \to 3\ell$ events. Since lower values of $m_{1/2}$ are preferred by fine-tuning arguments [36], there is a good chance Tevatron experiments could discover SUSY via 3ℓ events if nature chose this parameter set.

We also compare the results of Fig. 7 with expectations for supersymmetry at the CERN LHC collider. Of course, LHC experiments can cover the whole parameter plane up to $m_{1/2} \sim 600-800$ GeV with only $\int \mathcal{L} dt = 10$ fb⁻¹ of integrated luminosity, at $\sqrt{s} = 14$ TeV, via searches for multi-jet+ E_T events from gluino and squark cascade decays [30], so discovery of SUSY would be no problem. We also plot in Fig. 7 the contour beneath which sleptons ought to be visible at LHC [30,31]. We see that the cosmologically favored MDM region falls almost entirely within the slepton discovery region, so that if the MDM scenario is correct, then LHC has a very high probability to discover a slepton. Since sleptons are relatively light, LHC experiments ought as well to be sensitive to $\widetilde{W}_1\widetilde{Z}_2 \to 3\ell$ events over much, but not all, of the favored MDM region [30,31]. (In some of the favored region, $\widetilde{Z}_2 \to \nu \widetilde{\nu}$ or $\widetilde{Z}_1 h$, thus spoiling the signal.) Finally, since $m_{\tilde{\ell}} \lesssim 250$ GeV in the MDM scenario, sleptons would then likely be visible at a linear e^+e^- collider operating at $\sqrt{s} = 500$ GeV.

In Fig. 8, we show the same relic density contours as in Fig. 3 ($\tan \beta = 2$, $\mu > 0$), and compare again with expectations for colliders. In this case, we see the LEP2 contour again lies in a region of $\Omega h^2 < 0.15$, although it does encompass the cosmologically interesting region around ($m_0, m_{1/2}$) ~ (100, 110). The LEP2 Higgs contour in this case lies at $m_{1/2} \sim 170$ GeV, and thus covers only a portion of the MDM favored region. Thus, if the MDM scenario is correct, and $\tan \beta$ is small, minimal SUGRA sparticles or light Higgs boson might still not be accessible at LEP2. We also plot the contour due to the combined Tevatron MI reach. In this case, there is a large Tevatron reach due to $\widetilde{W}_1 \widetilde{Z}_2 \to 3\ell$ extending to $m_{1/2} \sim 230$ GeV, overlapping considerably with the MDM region. Finally, we note once

again that LHC can cover the whole plane via multi-jet+ E_T searches. In addition, the MDM region lies again almost entirely within the LHC slepton search region, and overlaps substantially with the LHC $\widetilde{W}_1\widetilde{Z}_2 \to 3\ell$ clean trilepton region [31].

Last of all, we turn to Fig. 9, which compares the neutralino relic density with collider search regions for large $\tan \beta = 10$, with $\mu < 0$. In this case, we note that the MDM favored region lies entirely above the region that is searchable at LEP2. In addition, for this case, the lightest Higgs boson has mass $m_h \gtrsim 90$ GeV throughout the plane, beyond the reach of LEP2 at $\sqrt{s} = 190$ GeV. Hence, if $\tan \beta$ is large, and the MDM scenario is correct, then there would be little hope of seeing SUSY at LEP2. In this case, the prospect for minimal SUGRA at Tevatron MI is even worse, except for the narrow region extending along $m_0 \sim 100$ GeV, which enters into the cosmologically favored MDM region. Finally, we note that once again the LHC slepton reach contour excloses most of the MDM region, with the main exception being the band of allowed MDM region extending to large m_0 along $m_{1/2} \sim 160 - 170$ GeV. The LHC $\widetilde{W}_1 \widetilde{Z}_2 \to 3\ell$ region encloses pieces of the MDM region, but leaves significant areas uncovered [31].

V. CONCLUSION

In this paper, working within the minimal supergravity model with radiative electroweak symmetry breaking and universal GUT scale soft supersymmetry breaking terms, we have evaluated the cosmological relic density from neutralinos produced in the early universe. Our technique was to evaluate all lowest order neutralino annihilation Feynman diagrams as complex helicity amplitudes. We then performed the necessary integrations numerically, preserving relativistic covariance, and avoiding the usual expansion as a power series in velocity. While this approach might be regarded as a brute force numerical calculation, it does include relativistic thermal averaging, annihilation threshold effects, and careful integration over Breit-Wigner poles. We do not include co-annihilation processes in our calculations, which are however unimportant within the SUGRA framework, in which we work.

Our numerical results for the neutralino relic density were presented in Figures 1-6. For the favored mixed dark matter scenario, for which $0.15 < \Omega h^2 < 0.4$, we find that, unless annihilation occurs via s-channel Z or h exchange (in which case $m_{\tilde{g}} < 300 - 400$ GeV [37]), $m_{\tilde{g}} \lesssim 1000$ GeV, and $m_{\tilde{\ell}} \lesssim 250$ GeV. The less conservative constraint from the age of the universe $(\Omega h^2 < 1)$ yields larger bounds on sparticle masses.

We also examined the implications of our relic density calculations for collider searches for the sparticles of minimal SUGRA. These results have been summarized in Figs. 7-9. Within the MDM range of Ωh^2 , we find that LEP2 has a high probability to detect a light Higgs boson if $\tan \beta$ is small and $\mu < 0$. For the opposite sign of μ , m_h can be larger, and detection at LEP2 is less certain. Prospects for detection of sleptons or charginos at LEP2 are less bright: generally, if $m_{\tilde{\ell}} < 90$ GeV, t-channel neutralino annihilation is too large, leading to rather low values of neutralino relic density. Likewise, if $m_{\widetilde{W}_1} < 90$ GeV, then $m_{\widetilde{Z}_1} \lesssim 45$ GeV, and neutralinos can annihilate via s-channel Z or h exchange, again leading to only a small relic abundance.

Prospects for discovering SUGRA at Tevatron MI experiments are somewhat brighter, since a reasonable relic density requires roughly $100 < m_{\tilde{\ell}} < 250$ GeV. Such a slepton mass

range generally leads to enhanced leptonic decays of neutralinos, giving Tevatron experiments a good chance to find SUGRA via $\widetilde{W}_1\widetilde{Z}_2 \to 3\ell$ searches.

The CERN LHC pp collider can make a thorough search for supersymmetry over all the allowed parameter space in the multi-jet $+E_T$ channel. However, the rather light slepton masses required for reasonable neutralino relic densities falls within the range of LHC experimental sensitivity, so there is a good chance to find sleptons at LHC if, for instance, the MDM scenario turns out to be correct. Likewise, experiments at an e^+e^- linear collider operating at $\sqrt{s} \sim 500$ GeV would stand a good chance of discovering sleptons, since they would be sensitive to slepton pair production for $m_{\tilde{\ell}} \lesssim 230$ GeV [38,39].

Note added: Upon completion of this work, a preprint appeared which addressed the neutralino dark matter relic density in SUGRA models with non-universal soft-breaking terms [40].

ACKNOWLEDGMENTS

We thank X. Tata and C. H. Chen for discussions, and X. Tata for comments on the manuscript. This research was supported in part by the U. S. Department of Energy under grant number DE-FG-05-87ER40319.

REFERENCES

- [1] For reviews of the MSSM, see H. P. Nilles, Phys. Rep. **110**, 1 (1984); H. Haber and G. Kane, Phys. Rep. **117**, 75 (1985); X. Tata, in *The Standard Model and Beyond*, p. 304, edited by J. E. Kim, World Scientific (1991).
- [2] S. Wolfram, Phys. Lett. B82, 65 (1979); C. B. Dover, T. K. Gaisser and G. Steigman,
 Phys. Rev. Lett. 42, 1117 (1979); P. F. Smith et. al., Nucl. Phys. B206, 333 (1982); E.
 Norman et. al., Phys. Rev. Lett. 58, 1403 (1987).
- [3] H. Baer, M. Drees and X. Tata, Phys. Rev. **D41**, 3414 (1990).
- [4] J. Ellis, D. Nanopoulos, L. Roszkowski and D. Schramm, Phys. Lett. **B245**, 251 (1990);
 L. Krauss, Phys. Rev. Lett. **64**, 999 (1990).
- [5] E. W. Kolb and M. S. Turner, *The Early Universe*, (Addison-Wesley, Redwood City, 1989).
- [6] G. Jungman, M. Kamionkowski and K. Griest, SU-4240-605 (1995), (submitted to Physics Reports); see also J. Ellis, CERN-TH.7083/93 (1993).
- [7] A. H. Chamseddine, R. Arnowitt and P. Nath, Phys. Rev. Lett. 49, 970 (1982);
 R. Arnowitt and P. Nath, Lectures presented at the VII J. A. Swieca Summer School, Campos do Jordao, Brazil, 1993 CTP-TAMU-52/93; Properties of SUSY Particles, L. Cifarelli and V. Khoze, Editors, World Scientific (1993); for a recent discussion, see e.g. M. Drees and S. Martin, in Electroweak Symmetry Breaking and Beyond the Standard Model, edited by T. Barklow, S. Dawson, H. Haber and J. Siegrist, (World Scientific, to be published).
- [8] K. Inoue, A. Kakuto, H. Komatsu and H. Takeshita, Prog. Theor. Phys. 68, 927 (1982) and 71, 413 (1984).
- [9] L. Ibañez and G. Ross, Phys. Lett. B110, 215 (1982); L. Ibañez, Phys. Lett. B118, 73 (1982); J. Ellis, D. Nanopoulos and K. Tamvakis, Phys. Lett. B121, 123 (1983); L. Alvarez-Gaumé, J. Polchinski and M. Wise, Nucl. Phys. B121, 495 (1983).
- [10] Some recent analyses of supergravity mass patterns include, J. Ellis and F. Zwirner, Nucl. Phys. B338, 317 (1990); G. Ross and R. G. Roberts, Nucl. Phys. B377, 571 (1992); R. Arnowitt and P. Nath, Phys. Rev. Lett. 69, 725 (1992); M. Drees and M. M. Nojiri, Nucl. Phys. B369, 54 (1993); S. Kelley et. al., Nucl. Phys. B398, 3 (1993); M. Olechowski and S. Pokorski, Nucl. Phys. B404, 590 (1993); V. Barger, M. Berger and P. Ohmann, ibid. 49, 4908 (1994); G. Kane, C. Kolda, L. Roszkowski and J. Wells, Phys. Rev. D49, 6173 (1994); D. J. Castaño, E. Piard and P. Ramond, Phys. Rev. D49, 4882 (1994); W. de Boer, R. Ehret and D. Kazakov, Karlsruhe preprint, IEKP-KA/94-05 (1994); H. Baer, C. H. Chen, R. Munroe, F. Paige and X. Tata, Phys. Rev. D51, 1046 (1995).
- [11] B. Lee and S. Weinberg, Phys. Rev. Lett. **39**, 165 (1977).
- [12] H. Goldberg, Phys. Rev. Lett. **50**, 1419 (1983).
- [13] J. Ellis, J. Hagelin, D. Nanopoulos and M. Srednicki, Phys. Lett. B127, 233 (1983);
 J. Ellis, J. Hagelin, D. Nanopoulos, K. Olive and M. Srednicki, Nucl. Phys. B238, 453 (1984);
 J. Ellis, J. Hagelin and D. Nanopoulos, Phys. Lett. B159, 26 (1985).
- [14] K. Griest, Phys. Rev. D38, 2357 (1988); K. Griest, M. Kamionkowski and M. Turner, Phys. Rev. D41, 3565 (1990).
- [15] K. Olive and M. Srednicki, Phys. Lett. **B230**, 78 (1989) and Nucl. Phys. **B355**, 208 (1991);
 J. MacDonald, K. Olive and M. Srednicki, Phys. Lett. **B283**, 80 (1992).

- [16] M. Nojiri, Phys. Lett. B261, 76 (1991); M. Drees and M. Nojiri, Phys. Rev. D47, 376 (1993).
- [17] J. Lopez, D. Nanopoulos and K. Yuan, Phys. Lett. B267, 219 (1991) and Nucl. Phys. B370, 445 (1992); S. Kelley, J. Lopez, D. Nanopoulos, H. Pois and K. Yuan, Phys. Lett. B273, 423 (1991).
- [18] J. Ellis and L. Roszkowski, Phys. Lett. B283, 252 (1992); L. Roszkowski and R. Roberts, Phys. Lett. B309, 329 (1993); G. Kane, C. Kolda, L. Roszkowski and J. Wells, Ref. [10].
- [19] R. Arnowitt and P. Nath, Phys. Rev. Lett. 70, 3696 (1993) and CTP-TAMU-53/94 (1994).
- [20] K. Griest and D. Seckel, Phys. Rev. **D43**, 3191 (1991).
- [21] P. Gondolo and G. Gelmini, Nucl. Phys. **B360**, 145 (1991).
- [22] H. Haber and R. Hempfling, Phys. Rev. Lett. 66, 1815 (1991); J. Ellis, G. Ridolfi and F. Zwirner, Phys. Lett. B257, 83 (1991); T. Okada, H. Yamaguchi and T. Tanagida, Prog. Theor. Phys. Lett. 85,1 (1991); we use the calculations of M. Bisset, U. of Hawaii Ph. D. thesis, UH-511-813-94 (1994), as implemented in ISAJET [34].
- [23] G. Gamberini, G. Ridolfi and F. Zwirner, Nucl. Phys. **B331**, 331 (1990).
- [24] J. Lopez, D. Nanopoulos, H. Pois, X. Wang and A. Zichichi, Phys. Rev. D48, 4062 (1993).
- [25] H. Baer, M. Brhlik, R. Munroe and X. Tata, FSU-HEP-950501 (1995).
- [26] H. Baer, C. Kao and X. Tata, Phys. Rev. D48, R2978 (1993) and Phys. Rev. D51, 2180 (1995).
- [27] J. Lopez, D. Nanopoulos, X. Wang and A. Zichichi, Phys. Rev. **D48**, 2062 (1993) and CERN-TH.7535/94; J. Lopez, D. Nanopoulos, G. Park, X. Wang and A. Zichichi, Phys. Rev. **D50**, 2164 (1994); T. Kamon, J. Lopez, P. McIntyre and J. T. White, Phys. Rev. **D50**, 5676 (1994).
- [28] H. Baer, C. H. Chen, C. Kao and X. Tata, Phys. Rev. **D52**, 1565 (1995).
- [29] S. Mrenna, G. Kane, G. Kribs and J. Wells, UM-TH-95-14 (1995).
- [30] H. Baer, C. H. Chen, F. Paige and X. Tata, Phys. Rev. **D49**, 3283 (1994), Phys. Rev. **D50**, 4508 (1994) and FSU-HEP-950204 (1995), Phys. Rev. **D** (in press).
- [31] C. H. Chen, Florida State University Ph. D. thesis FSU-HEP-950720 (1995).
- [32] H. Baer and X. Tata, Phys. Rev. **D47**, 2739 (1993).
- [33] See H. Baer, C. H. Chen, R. Munroe, F. Paige and X. Tata, Ref. [10].
- [34] F. Paige and S. Protopopescu, in *Supercollider Physics*, p. 41, ed. D. Soper (World Scientific, 1986); H. Baer, F. Paige, S. Protopopescu and X. Tata, in *Proceedings of the Workshop on Physics at Current Accelerators and Supercolliders*, ed. J. Hewett, A. White and D. Zeppenfeld, (Argonne National Laboratory, 1993).
- [35] HELAS: HELicity Amplitude Subroutines for Feynman Diagram Evaluations, H. Murayama, I. Watanabe and K. Hagiwara, KEK-91-11 (1992).
- [36] R. Barbieri and G. Giudice, Nucl. Phys. B306, 63 (1988); G. Anderson and D. Castaño, MIT-CTP-2369 (1994) presents an updated measure of fine-tuning, and associated bounds on sparticle masses.
- [37] H. Baer, M. Drees, C. Kao, M. Nojiri and X. Tata, Phys. Rev. **D50**, 2148 (1994).
- [38] T. Tsukamoto, K. Fujii, H. Murayama, M. Yamaguchi and Y. Okada, Phys. Rev. D51, 3153 (1995).

- [39] H. Baer et. al., in Electroweak Symmetry Breaking and Beyond the Standard Model, edited by T. Barklow, S. Dawson, H. Haber and J. Siegrist, (World Scientific, to be published), FSU-HEP-950401.
- [40] V. Berezinsky et. al., CERN-TH 95-206 (1995).

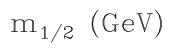
TABLES

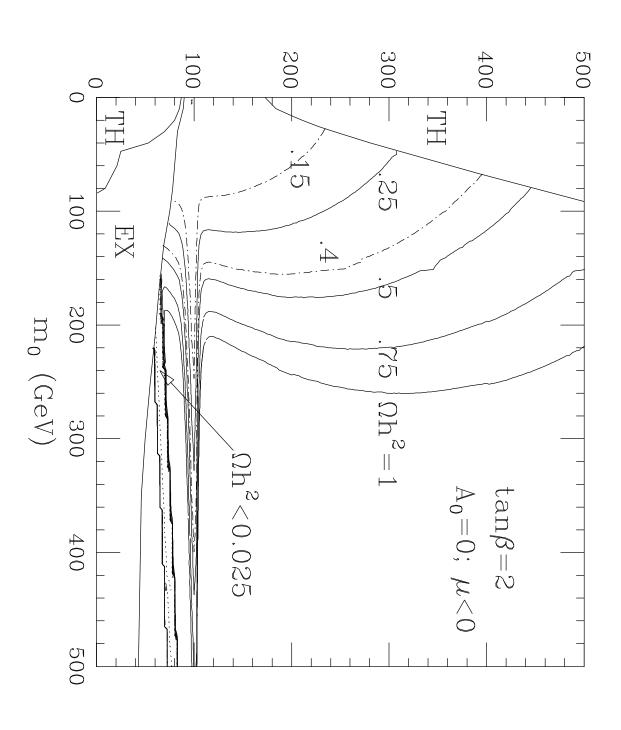
TABLE I. A tabulation of Feynman diagrams contributing to our neutralino annihilation cross section calculation.

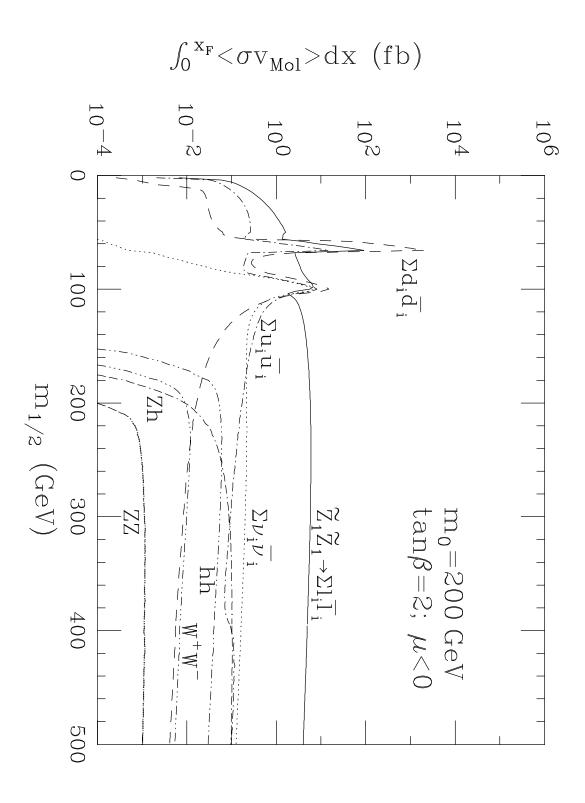
	Particles exchanged		
Process	s-channel	t-channel	u-channel
$\widetilde{Z}_1\widetilde{Z}_1 o Z^0Z^0$	h, H	$\widetilde{Z}_{1,2,3,4}$	$\widetilde{Z}_{1,2,3,4}$
$\widetilde{Z}_1\widetilde{Z}_1 \to W^+W^-$	h, H, Z^0	$\widetilde{W}_{1,2}^{\pm}$	$\widetilde{W}_{1,2}^{\pm}$
$\widetilde{Z}_1\widetilde{Z}_1 \to Z^0 h$	Z^0, A	$\widetilde{Z}_{1,2,3,4}$	$\widetilde{Z}_{1,2,3,4}$
$\widetilde{Z}_1\widetilde{Z}_1 \to Z^0H$	Z^0, A	$Z_{1,2,3,4}$	$\widetilde{Z}_{1,2,3,4}$
$\widetilde{Z}_1\widetilde{Z}_1 \to Z^0A$	h, H	$\widetilde{Z}_{1,2,3,4}$	$\widetilde{Z}_{1,2,3,4}$
$\widetilde{Z}_1\widetilde{Z}_1 \to W^-H^+$	h, H, A	$\widetilde{W}_{1,2}^{\pm}$	$\widetilde{W}_{1,2}^{\pm}$
$\widetilde{Z}_1\widetilde{Z}_1 \to W^+H^-$	h, H, A	$\widetilde{Z}_{1,2,3,4}$ $\widetilde{W}_{1,2}^{\pm}$ $\widetilde{W}_{1,2}^{\pm}$	$\widetilde{W}_{1,2}^{\pm}$
$\widetilde{Z}_1\widetilde{Z}_1 \to hh$	h, H	$\widetilde{Z}_{1,2,3,4}$	$\widetilde{Z}_{1,2,3,4}$
$\widetilde{Z}_1\widetilde{Z}_1 \to HH$	h, H	$\widetilde{Z}_{1,2,3,4}$	$\widetilde{Z}_{1,2,3,4}$
$\widetilde{Z}_1\widetilde{Z}_1 \to hH$	h, H	$\widetilde{Z}_{1,2,3,4}$	$\widetilde{Z}_{1,2,3,4}$
$\widetilde{Z}_1\widetilde{Z}_1 \to AA$	h, H	$\widetilde{Z}_{1,2,3,4}$	$\widetilde{Z}_{1,2,3,4}$
$\widetilde{Z}_1\widetilde{Z}_1 \to hA$	Z^0, A	$\widetilde{Z}_{1,2,3,4}$	$\widetilde{Z}_{1,2,3,4}$
$\widetilde{Z}_1\widetilde{Z}_1 \to HA$	h, H	$\widetilde{Z}_{1,2,3,4}$	$\widetilde{Z}_{1,2,3,4}$
$\widetilde{Z}_1\widetilde{Z}_1 \to H^+H^-$	h, H, Z^0	$W_{1,2}^{\pm}$ $\tilde{f}_{1,2}^{\pm}$	$\frac{\widetilde{W}_{1,2}^{\pm}}{\widetilde{f}_{1,2}^{\pm}}$
$\widetilde{Z}_1\widetilde{Z}_1 \to f\bar{f}$	Z^0, h, H, A	$\widetilde{f}_{1,2}^\pm$	$\widetilde{f}_{1,2}^\pm$

FIGURES

- FIG. 1. Plot of contours of constant Ωh^2 in the m_0 vs. $m_{1/2}$ plane, where $A_0 = 0$, $\tan \beta = 2$, $\mu < 0$ and $m_t = 170$ GeV. The regions labelled by TH (EX) are excluded by theoretical (experimental) considerations.
- FIG. 2. Relativistic thermally averaged cross section times velocity as a function of $m_{1/2}$, for $m_0 = 200$ GeV, with other parameters as in Fig. 1.
 - FIG. 3. Same as Fig. 1, except now $\mu > 0$.
- FIG. 4. Relativistic thermally averaged cross section times velocity as a function of $m_{1/2}$, for $m_0 = 200$ GeV, with other parameters as in Fig. 3.
 - FIG. 5. Same as Fig. 1, except now $\tan \beta = 10$.
- FIG. 6. Relativistic thermally averaged cross section times velocity as a function of $m_{1/2}$, for $m_0 = 200$ GeV, with other parameters as in Fig. 5.
- FIG. 7. Same as Fig. 1, except we also show the region below the contour labelled MI, which is accessible to Tevatron Main Injector era experiments, and the region below the LEP2 contour, where sparticles are accessible to experiments at LEP2 operating at $\sqrt{s} = 190$ GeV. Below the LEP2-Higgs contour, the lightest SUSY Higgs h is accessible at LEP2. Below the LHC contour, sleptons ought to be accessible to LHC experiments.
 - FIG. 8. Same as Fig. 7, except now $\mu > 0$.
 - FIG. 9. Same as Fig. 7, except now $\tan \beta = 10$.







$$m_{1/2}$$
 (GeV)

